Phase separation in lipid-based nanoparticles: exploring the nano-bio interface

Papadopoulou, P.

Appendix I

Protocol for *in situ* formation of gold nanoparticles in phase-separated liposomes

Herein, a protocol to achieve *in situ* formation of gold nanoparticles (AuNPs) inside the phase-separated PAP3 liposome core, is introduced. The protocol is adapted and modified from a previously described method.[1]

Materials

Tris(hydroxymethyl)aminomethane (Tris), Trisodium Citrate Dihydrate ($HOC(COONa)(CH_2COONa)_2 \cdot {}_2H_2O$), Gold(III) chloride trihydrate ($HAuCl_4 \cdot 3H_2O$) and 1,2-distearoyl-sn-glycero-3-phosphatidylcholine (DSPC) were purchased from Sigma Aldrich. DOaG was synthesized as described in Chapter 2 and in reference [2]. $HAuCl_4 \cdot 3H_2O$ was stored in a dark place.

Method

1. Tris buffer was prepared at 10 mM concentration and pH was adjusted to 7.4 with 1M HCl.
2. Using a volumetric flask (50 mL), an aqueous stock solution of 50.1 mM $HAuCl_4 \cdot 3H_2O$ was prepared immediately after opening the manufacturer's bottle (using all the content from the bottle). From this stock, a stock of 5 mM was prepared.
3. Using a volumetric flask (50 mL), an aqueous stock solution of 20.4 mM trisodium citrate dihydrate was prepared.
4. Individual lipids as stock solutions of DSPC and DOaG (10 mM) in chloroform, were combined in a glass vial to 1:1 molar ratio and dried to a thin film, first under N_2 stream, then >1 h under vacuum.
5. Lipid films were redissolved in 50 μL absolute ethanol with gentle vortexing if necessary, to a total lipid concentration of 50 mM.
6. Using the stock solutions prepared in steps 2 and 3 an queous solution of $HAuCl_4$: Sodium Citrate was prepared at a 1 : 4.08 ratio (Turkevich solution).[3] Two concentrations of $HAuCl_4$ have been successfully used: 1.75 mM or 2.5 mM. Turkevich solution is prepared fresh every time and is used immediately after preparation to ensure prevention of premature AuNP formation prior to liposome formation.
7. Using a (pre-heated) glass micro-syringe (Hamilton, syringe series 700, volume 50), 35.7 μL of the ethanolic lipid solution (warm after submersion in a water bath of 50 °C for 5 sec) was rapidly injected in a glass vial containing 2.5 mL of Turckevic solution (1:71 v/v; EtOH:Turkevich solution) submerged in a 50 °C water bath (freshly made and submerged only for ~2-3 min before injection), under constant vigorous stirring (650 rpm – stirring bar dimensions: 12 x 4 x 4 cm), to form large unilamellar vesicles.
8. Liposomal solution (2.5 mL) was immediately passed through a size exclusion chromatography column (Illustra™ NAP25, GE Healthcare, Thermofischer Scientific)

equilibrated with Tris buffer 10 mM pH = 7.4, to replace the unencapsulated Turkevic solution with buffer.

9. Liposomes encapsulating Turkevich solution in their core were then transferred in an eppendorf tube (1.5 mL) and placed in a thermomixer with a stable temperature at 75 °C for 10 min to ensure initiation of gold reduction from Au^{+3} to Au^{0} and subsequent nucleation and growth of AuNPs.
10. Liposomes containing formed AuNPs were transferred to a dialysis tube (Float-a-lyzer® G2, 1 mL capacity, 1000 kDa MWCO, Spectrum labs) and dialyzed against Tris buffer 10 mM pH = 7.4 overnight at 4 °C, to ensure complete removal of ethanol.
11. The hydrodynamic diameter and polydispersity index (PDI) of liposomes containing AuNPs were characterized by Dynamic Light Scattering (DLS) (Malvern Zetasizer Nano ZS). DLS measurements were carried out at room temperature in 10 mM Tris buffer (pH = 7.4) at a total lipid concentration of approx. 100 μM. Reported DLS measurements are the average of three measurements.
12. Liposomes containing AuNPs (3 μL) were applied to a freshly glow-discharged carbon 200 mesh Cu grid (Lacey carbon film, Electron Microscopy Sciences, Aurion, The Netherlands). Grids were blotted for 3 sec at 99% humidity in a Vitrobot plunge-freezer (FEI VitrobotTM Mark III, Thermo Fisher Scientific). Cryo-Transmission Electron Microscopy (cryo-TEM) images were collected on a Talos L120C (NeCEN, Leiden University) or a TITAN (Eindhoven University of Technology) operating respectively at 120 kV or 300kV. In the case of Talos, images were recorded manually at a nominal magnification of 17500x or 36000x yielding respectively a pixel size of 5.87 or 2.89 ångström (Å) at the specimen. In the case of TITAN, images were recorded manually at a nominal magnification of 24000x or 30000x yielding a pixel size of 3.87 or 2.81 ångström (Å) at the specimen, respectively.
13. Cryo-electron tomography (cryo-ET) was performed on a Talos L120C (NeCEN, Leiden University) operating at 120kV. Tomographic tilt series acquisition was performed with Tomo4 software from Thermo Fisher Scientific with a total electron dose of less than 100 e^{-}/nm^{2}. Alignment and reconstruction of the series were performed using IMOD.[4]
14. Liposomes containing AuNPs were concentrated up to 5 mM total lipid concentration (relevant for *in vivo* use) with a Vivaspin® 2 centrifugal concentrator (2 mL volume, 300k MWCO). Note: to prevent liposomes from aggregating, centrifugal forces were not used. Briefly, liposomes were transferred in the concentrator which was let in an upright position. Solvent was slowly removed by gravity and by occasional shaking.

Characterization

Size (nm)	PDI
157.7	0.301

Cryo-TEM images

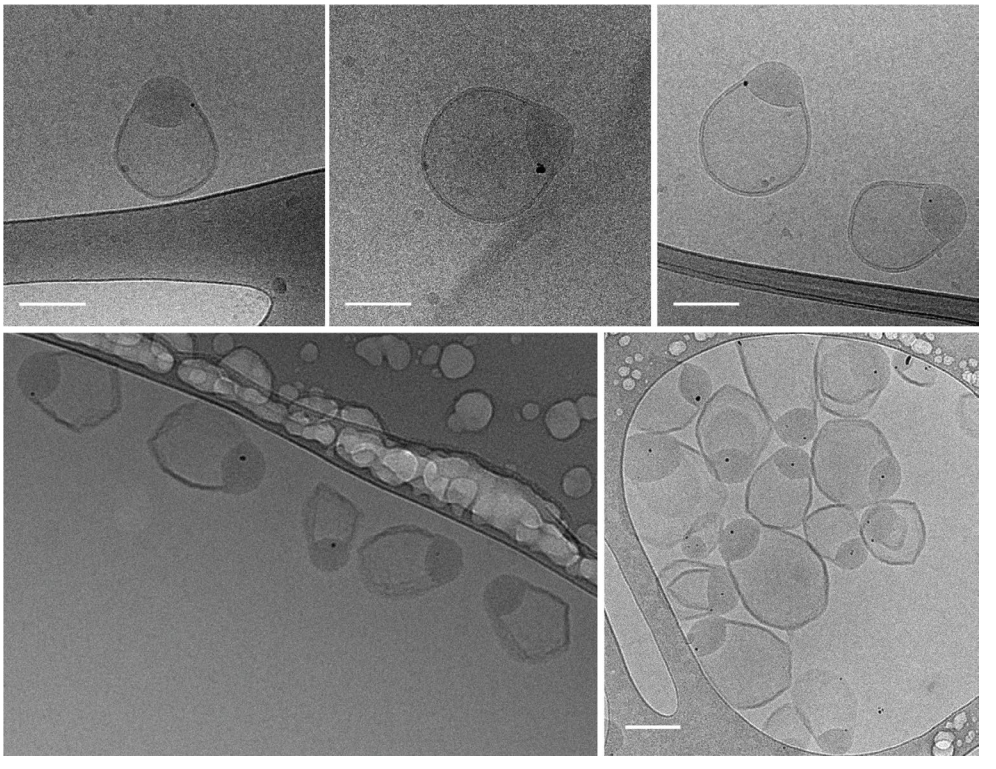

Figure 1: Cryo-TEM images depicting phase-separated PAP3 liposomes encapsulating AuNPs (black, electron dense dots) after *in situ* formation (Turkevich solution used: 1.75 mM $HAuCl_4$: 7.14 mM Sodium Citrate). Average AuNP size = 9.95 nm based on quantification (N = 103). Scale bars = 100 nm. Sample is free of unencapsulated AuNPs.

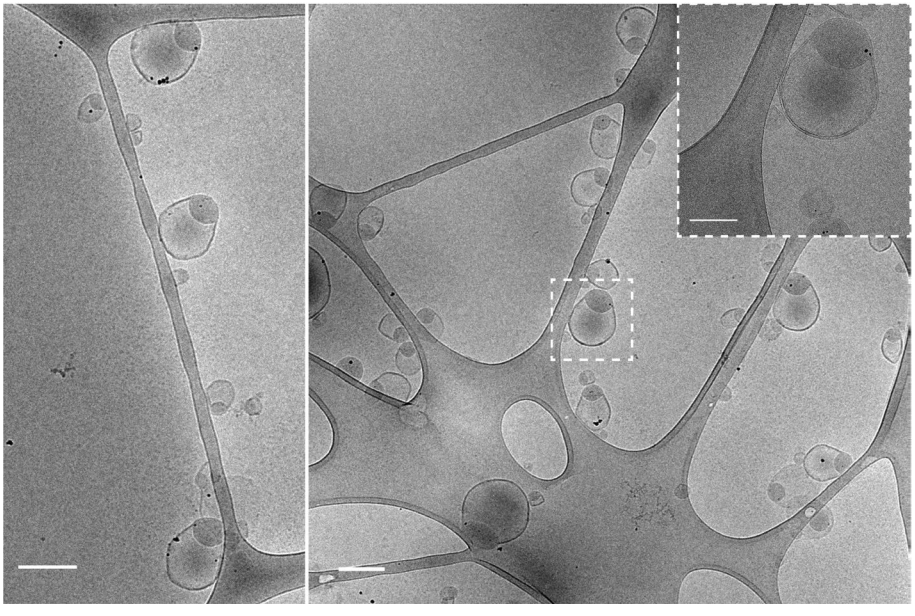

Figure 2: Cryo-TEM images depicting phase-separated PAP3 liposomes encapsulating AuNPs (black, electron dense dots) after *in situ* formation (Turkevich solution used: 2.5 mM $HAuCl_4$: 10.2 mM Sodium Citrate). Scale bars = 200 nm for low magnification images and 100 nm for insert. Sample is free of unencapsulated AuNPs.

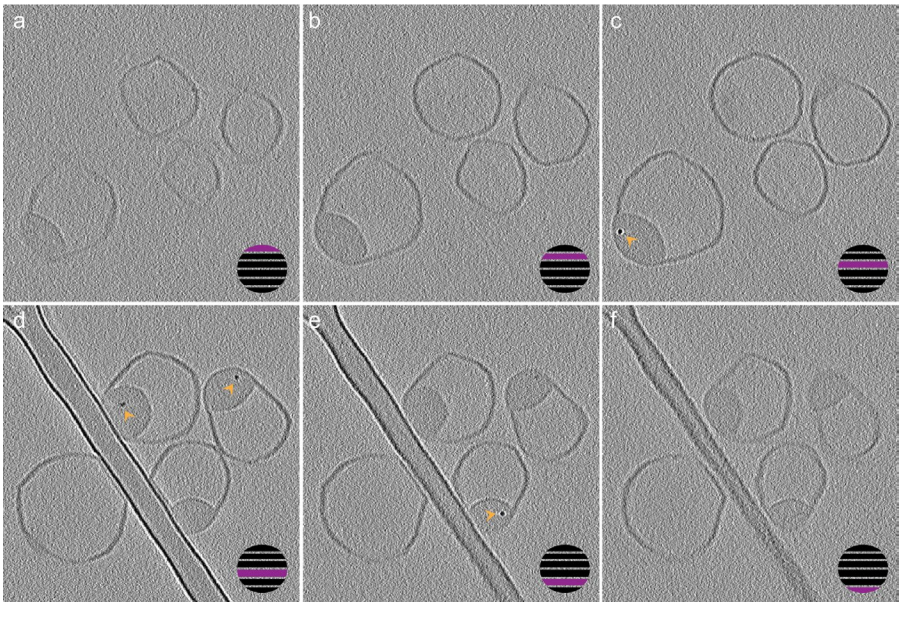

Figure 3. Cryo-electron tomography of PAP3 liposomes containing AuNPs. a-f) Representative slices of the tomogram showing AuNPs (orange arrows) reside in the inner

core of liposomes and show a preference for the liposome lipid droplet. Slice schematic (right bottom corner) shows which slice (in purple) corresponds to each image (a, f = top and bottom slices, b-e = middle slices). Turkevich solution used: 1.75 mM $HAuCl_4$: 7.14 mM Sodium Citrate.

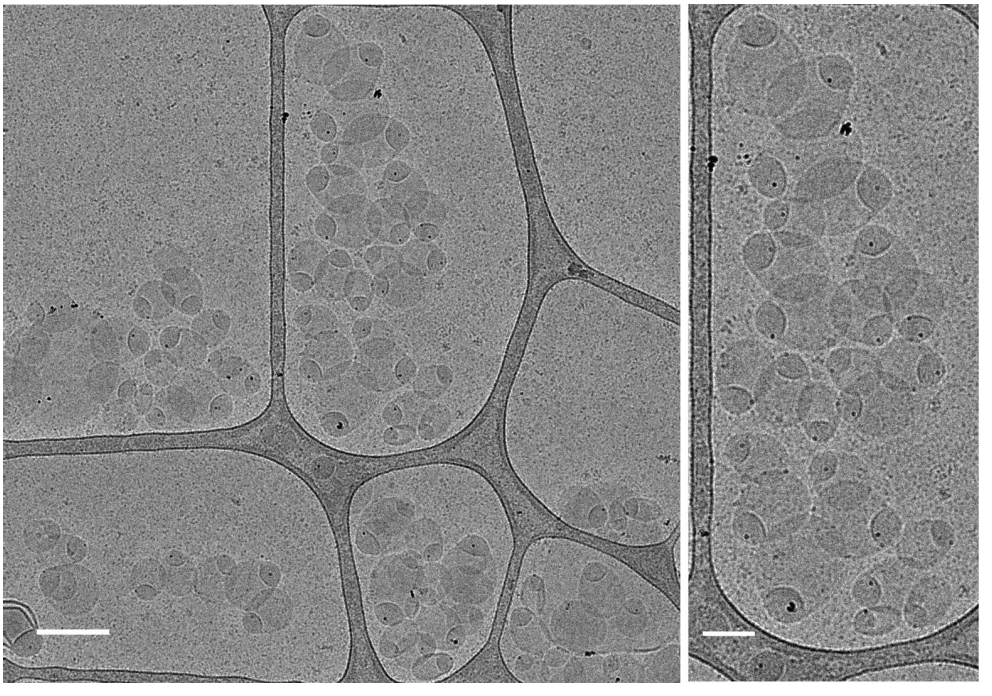

Figure 4. PAP3 liposomes containing AuNPs (black, electron dense dots) after incubation with human serum (1:1) for 10 min. Liposome morphology is preserved and AuNPs remain encapsulated (Turkevich solution used: 1.75 mM $HAuCl_4$: 7.14 mM Sodium Citrate). Average AuNP size = 9.62 nm based on quantification (N = 70). Scale bars = 200 nm for low magnification image and 100 nm for high magnification image.

References

1. Witzigmann, D.; Sieber, S.; Porta, F.; Grossen, P.; Bieri, A.; Strelnikova, N.; Pfohl, T.; Prescianotto-Baschong, C.; Huwyler, J. Formation of Lipid and Polymer Based Gold Nanohybrids Using a Nanoreactor Approach. *RSC Adv* **2015**, *5* (91), 74320–74328.
2. Arias-Alpizar, G.; Papadopoulou, P.; Rios, X.; Pulagam, K. R.; Moradi, M. A.; Pattipeiluhu, R.; Bussmann, J.; Sommerdijk, N.; Llop, J.; Kros, A.; Campbell, F. Phase-Separated Liposomes Hijack Endogenous Lipoprotein Transport and Metabolism Pathways to Target Subsets of Endothelial Cells In Vivo. *Adv Healthc Mater* **2023**, *12* (10), e2202709.
3. Turkevich, J.; Stevenson, P. C.; Hillier, J. A Study of the Nucleation and Growth Processes in the Synthesis of Colloidal Gold. *Discuss Faraday Soc* **1951**, *11*, 55–75.
4. Kremer, J. R.; Mastronarde, D. N.; McIntosh, J. R. Computer Visualization of Three-Dimensional Image Data Using IMOD. *J Struct Biol* **1996**, *116* (1), 71–76.

List of Abbreviations

apoAI apolipoprotein AI
apoCII apolipoprotein CII
ApoE apolipoprotein E
ASOs antisense oligonucleotides
Asp asparagine
ATTR transthyretin amyloidosis
BA basilar artery
BBB blood brain barrier
bECs brain endothelial cells
CE cholesteryl ester
CG coarse grained
CHO cholesterol
CHT caudal hematopoietic tissue
COM center of mass
CSF cerebrospinal fluid
CT computed tomography
CtA cerebral arteries
CV caudal vein
DAG diacylglycerol
DCM dichloromethane
DIPEA diisopropylethylamine
DLS dynamic light scattering
DLV dorsal longitudinal vein
DMAP dimethylaminopyridine
DMSO dimethylsulfoxide
DOaG dioleoylamidoglycerol
DODAP dioleoyldimethylammonium propane
DOE design of experiment
DOG dioleoylglycerol
DOPC dioleoylphosphatidylcholine
DOPS dioleoylphosphatidylserine
DOTMA dioctadecenyl-trimethylammonium propane
dpf days post fertilization
DSPC distearoylphosphatidylcholine
EL endothelial lipase
EMA European medicine agency
EPC phosphatidylcholine (egg)
EPG phosphatidylglycerol (egg)
EPR enhanced permeation-retention
ESI electron spray ionization
ET electron tomography
EV extracellular vesicle
FDA food and drug administration
FFA free fatty acid
FFT fast Fourier transform
GPIHBP1 lycosylphosphatidylinositol anchored high density lipoprotein binding protein 1
GUVs giant unilamellar vesicles
HDL high-density lipoprotein
H_{II} hexagonal phase
His histidine
HL hepatic lipase
hpi hours post injection
HRMS hight resolution mass spectrometry
HSPG heparan sulfate proteoglycans
ID injected dose
IV intravenous
KC Kupffer cells
L_d liquid disordered
LDL low-density lipoprotein
LDLr LDL receptor
LNP lipid nanoparticle

L_o	liquid ordered
LPL	lipoprotein lipase
LR	lissamine rhodamine
LSECs	liver sinusoidal endothelial cells
LUVs	large unilamellar vesicles
MCeV	middle cerebral vein
MD	molecular dynamics
MMCtA	mid.mesencephalic central artery
MPS	mononuclear phagocyte system
mRNA	messenger RNA
MS	mass spectrometry
MsA	mesencephalic artery
MsV	mesencephalic vein
NMR	nuclear magnetic resonance
NN	neural network
PBS	phosphate buffered saline
PC	phosphatidylcholine
PDI	polydispersity index
PEG	polyethylene glycol
PHBC	primordial hindbrain channel
PKC	protein kinase C
PMBC	primordial midbrain channel
PMF	potential mean force
POPC	palmitoyl-oleoyl-phosphocholine
RES	reticuloendothelial system
RNAi	RNA interference
rt	room temperature
SASA	solvent-accessible surface area
SEC	size exclusion chromatography
SECs	scavenging endothelial cells
Ser	serine
siRNA	small interfering RNA
SRB1	scavenger receptor B1
TEM	transmission electron microscopy
TG	triglyceride (or triacylglycerol)
TGL	triacylglycerol lipase
THF	tetrahydrofuran
TLC	thin layer chromatography
Trp	tryptophan
US	umbrella sampling
VLDL	very-low density lipoprotein
VLP	virus-like particle